

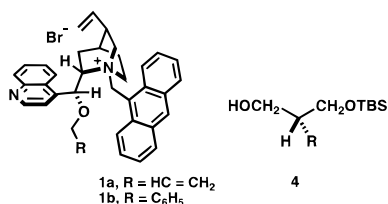
Highly Enantioselective Phase Transfer Catalyzed Alkylation of a 3-Oxygenated Propionic Ester Equivalent; Applications and Mechanism

E. J. Corey,* Yunxin Bo, and Jakob Busch-Petersen

Department of Chemistry and Chemical Biology
Harvard University, Cambridge, Massachusetts 02138

Received October 12, 1998

A detailed molecular mechanism has recently been described for the phase transfer catalyzed enantioselective alkylation of an enolate with use of the chiral quaternary cinchonidinium salt **1a**.^{1,2} This reaction was illustrated by a variety of examples in which a series of (*S*)- α -amino acid derivatives (both natural and unnatural) was prepared with enantioselectivities in the range 400:1 to 60:1 by alkylation of the *tert*-butyl glycinate–benzophenone Schiff base.³ In the mechanistic model contact ion pairing takes place selectively between the anionic oxygen of the enolate and just one of the tetrahedral faces of the cationic nitrogen of **1a** (for



steric reasons). In addition, considerable van der Waals attraction occurs between the enolate and a complementary binding site on the quaternary ammonium cation within the contact ion pair. The combination of electrostatic and van der Waals binding results in a highly structured contact ion pair in which only one face of the nucleophilic α carbon of the enolate is accessible to the electrophilic alkylating species.¹ This mechanistic picture provides a logical explanation for the absolute stereochemical course of the catalytic alkylation process and also the very high levels of enantioselectivity which are observed. In this paper we demonstrate that this remarkably enantioselective alkylation catalyst can be applied to other enolates and that the enantioselectivity varies in a predictable way with the electronic effect of remote substituents on the enolate. In addition, we present an analysis of the alkylation process that underscores the importance of charge density and entropy in determining the level of enantioselectivity.

The β,γ -unsaturated ester **2** was prepared from 4,4'-bis-(dimethylamino)benzophenone (Michler's ketone) by the following sequence: (1) reaction with γ -lithiated *tert*-butyl propiolate (from *n*-BuLi on the propiolate ester in THF at -78°C) in THF at -15°C for 20 h (68%); (2) catalytic reduction with 1 atm of H₂ over 5% Pd–BaSO₄ at 23°C for 20 min (91%); and (3) dehydration with CH₃SO₂Cl–Et₃N–4-*N,N*-(dimethylamino)-pyridine in CH₂Cl₂ at 0°C for 30 min (86%). Reaction of **2** in 1:1 CH₂Cl₂–Et₂O solution containing 10 mol % of chiral ammonium bromide **1b** with various alkyl bromides or iodides

Table 1. Enantioselective Catalytic Phase Transfer Alkylation

entry	RX ^a	Temp (°C) Time (h)	% Yield of 3 ^b	% ee ^c
1	CH ₃ I	-50, 12	68	98
2	CH ₃ (CH ₂) ₅ I	-45, 12	73	95
3	Cl(CH ₂) ₃ I	-45, 12	71	95
4	Cl(CH ₂) ₄ I	-45, 12	62	94
5		-65, 36	76	96
6	C ₆ H ₅ CH ₂ Br	-65, 36	83	94
7		-65, 12	81	98

^a An excess (*ca.* 5 equiv) of RX was employed. ^b Yields refer to chromatographically pure, isolated product **3**. ^c Enantiopurity of **3** was determined by chiral HPLC analysis (column: Regis Whelk-O1; elution solvent: 20% 2-propanol–hexane). In each case it was established by analysis of racemic **3** that the enantiomers were fully resolved.

in the presence of solid CsOH·H₂O proceeded smoothly to form the α alkylation product **3** in good yield and in high ee (94–98%), as summarized in Table 1. The (*R*)-absolute configuration for the alkylation products, which was predicted from the mechanistic model, was confirmed for the case of **3**, R = CH₃, by chemical correlation with (*R*)-(+)-2-methyl-3-*tert*-butyldimethylsilylpropane-1,3-diol (**4**, R = CH₃),⁴ [α]_D²⁵ +13.18 (*c* 0.19, CHCl₃), using the following sequence: (1) reduction of CO₂*t*-Bu to CH₂OH with diisobutylaluminum hydride in CH₂Cl₂ at $-78 \rightarrow 0^\circ\text{C}$ over 30 min; (2) silylation with *tert*-butyldimethylsilyl chloride (TBSCl)–Et₃N–DMF at 23°C for 1 h; (3) oxidation of C=C with catalytic OsO₄ and stoichiometric *N*-methylmorpholine *N*-oxide (NMO) in 8:1 acetone–H₂O at 23°C for 24 h; (4) oxidative C–C cleavage with Pb(OAc)₄ in CH₂Cl₂ at 0°C for 1 h; and (5) reduction of CHO to CH₂OH with NaBH₄ in CH₃OH at -40°C . In an analogous manner **4**, R = C₆H₅CH₂, *o*-C₆H₅-C₆H₄, R = *n*-C₆H₁₃ were synthesized in good overall yield from **3**, R = C₆H₅CH₂, *o*-C₆H₅C₆H₄, and *n*-C₆H₁₃, respectively. Thus a range of chiral 2-substituted monoprotected propane-1,3-diols, versatile building blocks for enantioselective synthesis, can be accessed by enantioselective phase transfer catalyzed conversion of **2** to **3**.

The general catalytic enantioselective conversion **2** \rightarrow **3** has a variety of potential applications other than to the synthesis of chiral propane-1,3-diol derivatives, especially when a bifunctional alkylating agent is used. Thus, starting with **3**, R = (CH₂)₃Cl, the chiral tetrahydropyran **5** was produced by (1) reduction of CO₂*t*-Bu to CH₂OH (DIBAL-H, CH₂Cl₂, -78 to 0°C for 30 min, 96%) and (2) cyclization (NaH, DMF, Bu₄NI at 23°C for 2 h, 92%). Two-step oxidative cleavage of the double bond of **5** (first cat. OsO₄–NMO, then Pb(OAc)₄, as above) afforded the aldehyde **6**, which was converted sequentially to the corresponding alcohol

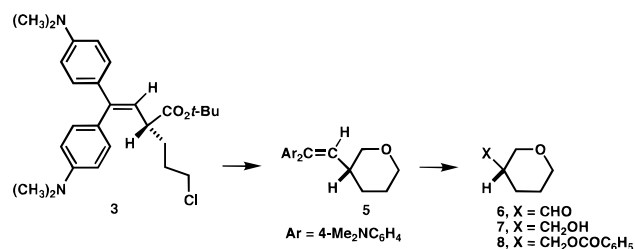
(4) (a) Harada, T.; Hayashiya, T.; Wada, I.; Iwa-ake, N.; Oku, A. *J. Am. Chem. Soc.* **1987**, *109*, 527. (b) Ihara, M.; Takahashi, M.; Taniguchi, N.; Yasui, K.; Fukumoto, K.; Kametani, T. *J. Chem. Soc. Perkin Trans. 1* **1989**, 897. (c) Marshall, J. A.; Trometer, J. D.; Cleary, D. J. *Tetrahedron* **1989**, *45*, 391.

(1) Corey, E. J.; Xu, F.; Noe, M. C. *J. Am. Chem. Soc.* **1997**, *119*, 12414.
(2) Corey, E. J.; Noe, M. C.; Xu, F. *Tetrahedron Lett.* **1998**, *39*, 5347.
(3) (a) Dolling, U.-H.; Davis, P.; Grabowski, E. J. *J. Am. Chem. Soc.* **1984**, *106*, 446. (b) Hughes, D. L.; Dolling, U.-H.; Ryan, K. M.; Schoenewaldt, E. F.; Grabowski, E. J. *J. Org. Chem.* **1987**, *52*, 4745. (c) O'Donnell, M. J.; Bennett, W. D.; Wu, S. *J. Am. Chem. Soc.* **1989**, *111*, 2353. (d) O'Donnell, M. J.; Wu, S.; Huffman, J. C. *Tetrahedron* **1994**, *50*, 4507. (e) Lipkowitz, K. B.; Cavanaugh, M. W.; Baker, B.; O'Donnell, M. J. *J. Org. Chem.* **1991**, *56*, 5181. (f) O'Donnell, M. J. et al. U.S. Patent 5,554,753, September 10, 1996. (g) O'Donnell, M. J.; Esikova, I. A.; Mi, A.; Shullenberger, D. F.; Wu, S. In *Phase-Transfer Catalysis*; Halpern, M. E., Ed.; ACS Symp. Ser. No. 659; American Chemical Society: Washington, DC, 1997; Chapter 10.

Table 2. Relationship between Enantioselectivity (er or ee) and Structure for the Allylation of $\text{Ar}_2\text{C}=\text{CHCH}_2\text{CO}_2t\text{-Bu}$ Catalyzed by Chiral Reagent **1b** and $\text{CsOH}\cdot\text{H}_2\text{O}$ at -65°C in 1:1 $\text{CH}_2\text{Cl}_2\text{-Et}_2\text{O}$

	1 , Ar =			
	C_6H_5	4- <i>t</i> -Bu C_6H_4	4-MeOC $_6\text{H}_4$	4-Me $_2\text{NC}_6\text{H}_4$
σ_p	0	-0.15	-0.28	-0.63
ee	67%	81%	91%	96%
er	5.1	9.5	21.2	49

7 and its benzoate **8** by conventional steps (72% yield of **8** overall from **5**).



Replacement of the *N,N*-dimethylamino substituents in the substrate **2** by less strongly electron-donating groups diminishes enantioselectivity, as shown in Table 2. In general, enantioselectivity correlates with Hammett σ constants such that it seems clear that the enantioselective pathway has a considerably more negative ρ value (by ca. -0.7) than the nonenantioselective reaction mode(s). The beneficial effect of electron-donating para substituents in $\text{Ar}_2\text{C}=\text{CHCH}_2\text{CO}_2t\text{-Bu}$ on the enantioselectivity of alkylation under control of the chiral quaternary ammonium ion **1b** is readily understood on the basis of the contact ion pair model,¹ since such substituents serve to increase electron density/charge on the enolate oxygen of the conjugate base of **2**. The effect of such negative charge enhancement is to strengthen the Coulombic force between the counterions and to favor very tight contact ion pairing. Clearly, the tighter the ion pairing, the greater the enantioselectivity of the alkylation **2** \rightarrow **3**. The structure of the ordered contact ion pair is depicted in Figure 1. With the enolate oxygen from **2** at closest approach ($d = \text{ca. } 3.5 \text{ \AA}$)¹ to the sterically least encumbered face of the N^+ center in **1b**, the enolate nestles well in the binding pocket formed by the rigid cation structure so that only the *re* face of the α carbon of the enolate is available for electrophilic attack, thus leading to the observed (*R*) products **3**.

To the extent that the structured tight ion pair of **1b** and the enolate of **2** (Figure 1) reduces the entropy of motion of the enolate component relative to the solvent separated/solvated

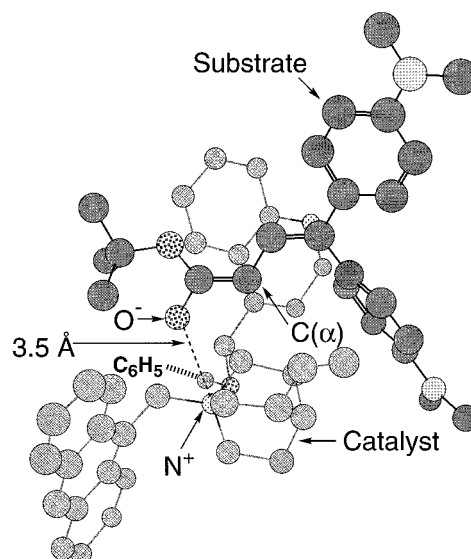


Figure 1. Structured contact ion pair derived from quaternary ammonium ion **1b** and the enolate derived from **2**. The *tert*-butyl group of **2** fits into the space between C(6)–C(8) of the quinoline ring and C(1)–C(2) of the anthracenyl group. The lower 4-Me $_2\text{NC}_6\text{H}_4$ group, which is *trans* to the β -C–H of the enolate, is perpendicular to the enolate σ -plane and fits into the space between the vinyl group, the quinuclidine ring, and positions N(1) and C(2) of the quinoline ring.

enolate, there could also be a more favorable entropy of activation for alkylation of the tightly held enolate vs the solvent separated/solvated enolate. This entropic effect would further enhance the reaction flux via the structured tight ion pair because of a smaller decrease in entropy of motion for the tight ion pair when the enolate and the alkyl halide are lined up in the stereoelectronically and sterically most favorable transition-state geometry.

The synthetic transformations described herein provide new insights into the developing area of catalytic enantioselective phase transfer reactions and a new methodology for the synthesis of a variety of chiral building blocks.

Acknowledgment. This research was supported by grants from the National Institutes of Health and the National Science Foundation.

Supporting Information Available: Experimental procedures (16 pp). See any current masthead page for ordering information and Web access instructions.

JA9835739